[CANCER RESEARCH 64, 6050–6057, September 1, 2004]

Hath1, Down-Regulated in Colon Adenocarcinomas, Inhibits Proliferation and Tumorigenesis of Colon Cancer Cells

Ching Ching Leow, Maria S. Romero, Sarajane Ross, Paul Polakis, and Wei-Qiang Gao

Department of Molecular Oncology, Genentech, Inc., South San Francisco, California

ABSTRACT

A striking feature of colon tumors is the significant reduction of goblet cells. Although targeted deletion of *Math1* in mice leads to a loss of intestinal secretory cells, including goblet cells, the role of *Hath1* in colon tumorigenesis remains unknown. Here we report that *Hath1*, the human ortholog of *Math1*, was dramatically down-regulated in colon tumor samples and colon cancer cell lines. Overexpression of Hath1 in HT29, an aggressive colon cancer cell line, resulted in a significant inhibition on cell proliferation, anchorage-independent growth in soft agar and, more importantly, growth of human colon cancer cell xenografts in athymic nude mice. Such inhibition was accompanied by altered expression of a goblet cell differentiation marker, MUC2, and cell cycle regulators cyclin D1 and $p27^{kip1}$. Hath1 expression also was up-regulated on inhibition of the Wnt pathway, which has been well implicated in colon tumorigenesis. Hence, this study suggests that Hath1 may be a novel factor downstream of the Wnt pathway capable of suppressing anchorage-independent growth of colon cancer cell lines. More importantly, this study is the first to establish a link between down-regulation of Hath1 expression and colon tumorigenesis.

INTRODUCTION

Colorectal cancer is the second leading cancer to afflict men and women in the United States (1, 2). Deregulation of the colonic mucosal homeostatic environment is one of the earliest signs of tumorigenesis. This process normally involves expansion of the proliferative crypt compartment accompanied by a delay or inhibition in cellular differentiation and apoptosis (3). Goblet cells represent one of the major populations of differentiated cells in the colonic mucosa. The majority of colorectal carcinoma is moderately well differentiated, which possess few mucin-secreting goblet cells. However, there is a rare subset of colorectal carcinoma that overproduces mucin (4–7). Hence, deregulation of differentiation and renewal of goblet cells, which is the major cell type responsible for secretion of mucins, may have a critical effect on colon cancer progression. Consistent with such observations, mice lacking the *mucin-2* (*Muc2*) gene reportedly developed intestinal adenomas (8), thus further stressing the importance of the mucinous secretions by goblet cells.

Hath1, a basic helix-loop-helix (bHLH) transcription factor homologous to the *Drosophila atonal* and mouse *Math1* (9), is a critical positive regulator of terminal cell differentiation (10–12). Targeted deletion of *Math1* reportedly results in failure of intestinal secretory cells, including goblet cells, to differentiate (13). Previous studies in the developing brain and inner ear also have shown that cerebellar granule neurons and inner ear hair cells fail to differentiate in the *Math1* knockout mice, respectively (14, 15). More importantly, misexpression of Math1 in postnatal and adult mammalian inner ears is capable of inducing terminal differentiation of inner ear hair cells (16–18). However, a potential role for Hath1 in colon cancer is yet unclear and remains to be determined.

In a majority of colon cancers, constitutive activation of the canonical Wnt signaling pathway often is a result of stabilization and accumulation of nuclear β-catenin. This buildup of nuclear β-catenin can occur through loss of adenomatous polyposis coli function, inactivation of Axin, or activating mutations in β-catenin (reviewed in refs. 19–21). Given the polygenic cause of most cancers, subsequent activation of oncogenes, such as K-*ras*, or inactivation of tumor suppressors, such as *p53*, have been shown. Several other genes, including *Cox-2*, *EGFR*, and *TGFβ*, have been identified as contributing factors to the multistage process of colon tumor progression (reviewed in ref. 22). Deregulated expression of genes involved in cell cycle regulation, such as *cyclin D1*, *p21*, and *p27*, also has been implicated in colon cancer (23–26). Therefore, the preceding list is not exhaustive, and more efforts are still needed to identify additional molecular targets that are deregulated during the malignant transformation of normal colonic mucosa.

In the present study, we hypothesize that Hath1 has suppressor effects on colon tumorigenesis. We observed Hath1 down-regulation in human colon adenocarcinoma samples. In addition to *in vitro* and *in vivo* studies of Hath1-suppressive effects on tumor cell proliferation, we also show that *Hath1* could potentially be a novel gene downstream of Wnt signaling.

MATERIALS AND METHODS

Cell Culture, Cell Transfection, and Tritiated-Thymidine Incorporation Assay. Colorectal cancer cell line HT29 was maintained under conditions as suggested by American Type Culture Collection (Manassas, VA). Cell transfection was performed with GenePorter (Gene Therapy Systems, San Diego, CA) according to manufacturer's instructions using 1 μg of pcDNA3.1 or pcDNA3.1 Hath1 DNA. After 24 hours, G418 was added to the media (400 μg/mL), and drug selection was continued for 2 weeks. Two colonies were randomly selected from each transfection for additional characterization. To measure DNA synthesis, an identical number of cells (4×10^3/well) were plated in 96-well plates in serum-free media. Twenty-four hours after cells were split, [^{3}H]thymidine (0.5 μCi/well) was added to the culture. After 16 hours of thymidine incorporation, trypsin (1 mg/mL) was added to each well for 30 minutes at 37°C before harvesting with a Packard cell harvester (Packard Instrument Company, Downers Grove, IL). Cpm/well then were counted with TOPCOUNT, a microplate scintillation counter (Packard Instrument Company). Data were collected from 24-culture well cell lines expressing pcDNA3.1 and pcDNA3.1 Hath1, respectively. Two-tailed, unpaired *t* test was used for statistical analysis, and results were expressed as mean ± SD.

Bromodeoxyuridine Immunofluorescent Staining. For bromodeoxyuridine (BrdUrd) immunofluorescence analysis, pcDNA3.1 and pcDNA3.1 Hath1 stably transfected HT29 cells were cultured on LabTek slides; Nunc (Rochester, NY). BrdUrd was added 3 hours before fixation. These cells initially were fixed [4% paraformaldehyde and 0.1 mol/L sodium phosphate buffer (pH 7.4)] for 30 minutes and subsequently treated with 2N HCl for 40 minutes at room temperature. After rinsing with 1× PBS, cells were blocked with 10% normal donkey serum (0.2% Triton X-100, 1× PBS) for 2 hours before incubation with a combination of mouse anti-BrdUrd antibody (1:40; Becton Dickinson, Franklin Lakes, NJ) in 3% normal donkey serum (0.2% Triton X-100, 1× PBS) overnight at 4°C. Positive staining was visualized by incubation with rhodamine-conjugated donkey antimouse secondary antibodies. Finally, cultures were mounted in VectaShield with 4′,6-diamidino-2-phe-

Received 1/28/04; revised 4/28/04; accepted 6/24/04.

The costs of publication of this article were defrayed in part by the payment of page charges. This article must therefore be hereby marked *advertisement* in accordance with 18 U.S.C. Section 1734 solely to indicate this fact.

Note: Supplementary data for this article can be found at Cancer Research Online (http://cancerres.aacrjournals.org).

Requests for reprints: Wei-Qiang Gao, Department of Molecular Oncology, MS #72, Genentech, Inc., 1 DNA Way, South San Francisco, CA 94080. Phone: 650-225-8101; Fax: 650-225-6240; E-mail: gao@gene.com.

nylindole (DAPI; Vector Labs, Burlingame, CA) and subsequently viewed using a Zeiss Axiophot epifluorescent microscope (Oberkochen, Germany). Images were captured with Compix imaging systems (Tualatin, OR) using a cooled CCD camera and analyzed using Adobe PhotoShop (Adobe Systems Inc., San Jose, CA). Cell counts were performed using captured micrograph images. For BrdUrd labeling index, BrdUrd-labeled cells *versus* the total number of DAPI-positive cells were counted. Fifteen different fields were randomly selected for analysis from three different plates. Data were presented as mean ± SD, and two-way, unpaired Student *t* test was used for statistical analysis.

Immunohistochemical and Histochemical Analysis of Paraffin Tissue Sections. Paraffin sections from Zymed MaxArrays (South San Francisco, CA) were deparaffinized through two washes of xylene and hydrated through an ethanol gradient. Sections then were left in 1× PBS for 5 minutes before antigen retrieval for 15 minutes in a pressure cooker (Cell Marque, Hot Springs, AR) with Delcere antigen retrieval solution (Cell Marque). Sections then were rinsed in 1× PBS and blocked in 10% normal donkey serum (0.2% Triton X-100 and 1× PBS) for 2 hours at room temperature. For immunohistochemistry, peroxidase block (Dako, Glostrup, Denmark) was applied before blocking with donkey serum. The primary antibodies used were rabbit anti-Math1 (1:100; Abcam, Cambridge, UK) and rabbit anti-MUC2 (1:100; Abcam). Rabbit anti-Math1 antibody from Chemicon (1:50; Temecula, CA) showed the same staining pattern as anti-Math1 antibody from Abcam (1:50; data not shown). Anti-Math1 was detected with ready-to-use biotinylated anti-rabbit secondary antibody (Dako). Anti-MUC2 was detected using donkey anti-rabbit Texas Red conjugated antibody (1:100; Jackson ImmunoResearch, West Grove, PA). For double-labeling studies, anti-Math1 antibody was detected with anti-rabbit Alexa-488 (1:500; Molecular Probes, Eugene, OR), and anti-Ki67 (1:25; Becton Dickinson) was detected with antimouse Alexa-594 (1:500; Molecular Probes). H&E staining (Vector Lab) was performed on sections after hydration through ethanol gradient, and sections were accordingly dehydrated through an ethanol gradient and xylene. H&E-stained sections were mounted using Histomount (Zymed).

Alcian Blue Staining. Paraffin sections were deparaffinized through two washes of xylene and hydrated through an ethanol gradient. Hydrated sections were left in distilled water before treating with 3% acetic acid for 3 minutes. Sections then were immersed in Alcian blue solution (pH 2.5; ScyTek, Logan, UT) and microwaved at high power for 30 seconds. After rinsing with running distilled water, nuclear fast red staining (Vector Lab) was carried out for 5 minutes, and sections then were washed with tap water. Finally, sections were dehydrated through ethanol gradient, cleared in xylene, and coverslipped with Histomount (Zymed).

Bioinformatics Analysis of Gene Logic Database. Gene Logic database is an archive of gene expression data collected from Affymetrix (Santa Clara, CA) microarray analysis of various tissues. Tissue samples from various normal and tumor tissues were processed using standard TRIzol, and RNeasy column method to extract RNA used generating cRNAs, which were later used for hybridizing to the latest version of the Affymetrix U-133 GeneChip. Results from those microarray experiments were compiled into a searchable database consisting of quantitative measurements of gene expression results from each normal or tumor tissue analyzed.

Gene Expression Analysis by TaqMan Reverse Transcription-PCR. Total RNA was prepared through CsCl extraction from matched colon tissue, and colon adenocarcinoma tissue samples were obtained from 12 different patients. RNA was isolated from 14 different colon cancer cell lines using RNeasy kit (Qiagen, Hilden, Germany). TaqMan real-time quantitative PCR analysis was performed as described previously (16, 27). The following specific probes and primers were used for Hath 1: probe, CTGCGCAATGTTATCCCGTCGTTCAA; forward primer, CAGAAGCAGAGACGGCTAGCA; and reverse primer, GGTCTCATATTTGGACAGCTTCTTGT; RPL19: probe, CACAAGCTGAAGGCAGACAAGGCCC; forward primer, GCGGATTCTCATGGAACACA; and reverse primer, GGTCAGCCAGGAGCTTCTTG); and MUC2: probe, CCTCCTAAGCTCGGCTTCCTCTCTTCAGATA; forward primer, CACACACCTACACCCACATCGA; and reverse primer, TTTATTATTGGAAAGCAAGGACTGAAC. Expression levels of genes of interest were normalized to *RPL19*. Initial real time-PCR amplifications also were examined by agarose gel electrophoresis to ensure that bands were only visible at the expected molecular weights. Data were collected from four cultures from each of the experimental groups and were expressed as mean ± SD.

Colony Formation Assay and Xenograft Experiment. Assays to determine colony formation in soft agar by tumor cell lines were performed using 60-mm tissue culture dishes containing a bottom layer consisting of 4 mL culture medium containing 0.5% (w/v) Agarplaque (BD PharMingen, San Diego, CA) and a top layer of 0.25% (w/v). Aliquots of pCDNA3.1 and pCDNA3.1 Hath1 stably transfected HT29 cells were plated at a density of 5000 cells/plate between the two layers of agar, and experiments were performed in triplicate. All of the visible colonies were counted after 2 weeks of incubation by taking micrographs from 16 randomly selected fields. Data collected from each experimental group were expressed as mean ± SD, and two-tailed, unpaired *t* test was used for statistical analysis. For HT29 colon cancer cell xenograft experiments, five female *nu/nu* nude mice (ages 6 to 8 weeks; Charles Rivers Laboratories, Wilmington, MA) were inoculated s.c. with 5×10^6 HT29 cells per group. The five groups consist of untransfected HT29, clones 2 and 3 of pcDNA3.1, and clones 4 and 9 of pcDNA3.1 Hath1. Tumor volume was calculated based on two dimensions, measured using calipers, and was expressed in cubic millimeters according to the formula: $V = 0.5a \times b^2$, where a and b are the long and the short diameters of the tumor, respectively. Data collected from each experimental group were expressed as mean ± SEM, and ANOVA statistical analysis was used. Mice were monitored for 32 days after inoculation, and tumor measurements were taken on day 5, 8, 13, 20, and 32. Mice were euthanized before tumor volumes reached 2000 mm^3 or when tumors showed signs of impending ulceration. This study was conducted in accordance with Animal Care Committee at Genentech, Inc.

Luciferase Assay. HT29 cells were transfected with 1 μg of pcDNA3, pcDNA3 APC2, and pcDNA3 $Lef1^{DN}$, 0.25 μg of renilla luciferase (pRL-SV40), and 0.75 μg of pTopflash using GenePorter (Gene Therapy Systems) according to manufacturer's instructions. Cells were harvested 48 hours later. Luciferase activity in 10 μL of lysate was analyzed in duplicate using the Promega Dual-Luciferase Reporter Assay System (Madison, WI) and a Tropix TR717 microplate luminometer (Applied Biosystems, Foster City, CA).

Western Blot Analysis. Cells were lysed with 2× protein lysis buffer [40 mmol/L Tris (pH 8.0), 270 mmol/L NaCl, 0.1 mol/L EGTA, 2% Triton X-100, 20% glycerol, and 0.3 mol/L magnesium chloride) containing complete MINI (Roche, Basel, Switzerland) protease inhibitors. Protein lysate was loaded onto SDS-PAGE gel with Laemmli loading buffer (Bio-Rad, Hercules, CA) and transferred onto polyvinylidene difluoride membrane. Blots then were blocked in 5% nonfat block (Bio-Rad) and incubated with primary antibody and then secondary antibody in 1% nonfat block. Positive antibody binding was detected using enhanced chemiluminescence according to manufacturer's instructions (Amersham, Piscataway, NJ). The membranes were probed with primary antibodies against MUC2 (1:200; Lab Vision, Fremont, CA), p27 (1:200; Lab Vision), and cyclin D1 (1:200; Santa Cruz Biotechnology, Santa Cruz, CA).

RESULTS

Goblet Cell Population Is Dramatically Reduced in Colon Adenocarcinomas. To confirm that there is a reduction in goblet cell population in colon tumors, Zymed human tissue microarrays containing sections of colon tumor with matched normal samples were examined for the presence of goblet cells. Each slide contains three types of sections from 18 individual colon adenocarcinoma cases. The three types of sections are from the colon adenocarcinoma tissue, the colon adjacent to the cancer, and a normal colon epithelium remote from the colon adenocarcinoma. In normal colon, goblet cells have a goblet-like morphology readily identifiable by H&E staining (black arrowhead, Fig. 1*A*). Sections obtained from colon adenocarcinoma display cells that appeared crowded without goblet-like features (Fig. 1*B*). We used Alcian blue staining to detect acidic mucins (28). The contents of goblet cells from normal colon appeared blue on staining with Alcian blue, thus, positively staining for the acidic mucins secreted by goblet cells (black arrowhead, Fig. 1*C*). Conversely, no Alcian blue-positive cells were visible in sections obtained from colon adenocarcinoma (Fig. 1*D*). Because MUC2 is uniquely produced by

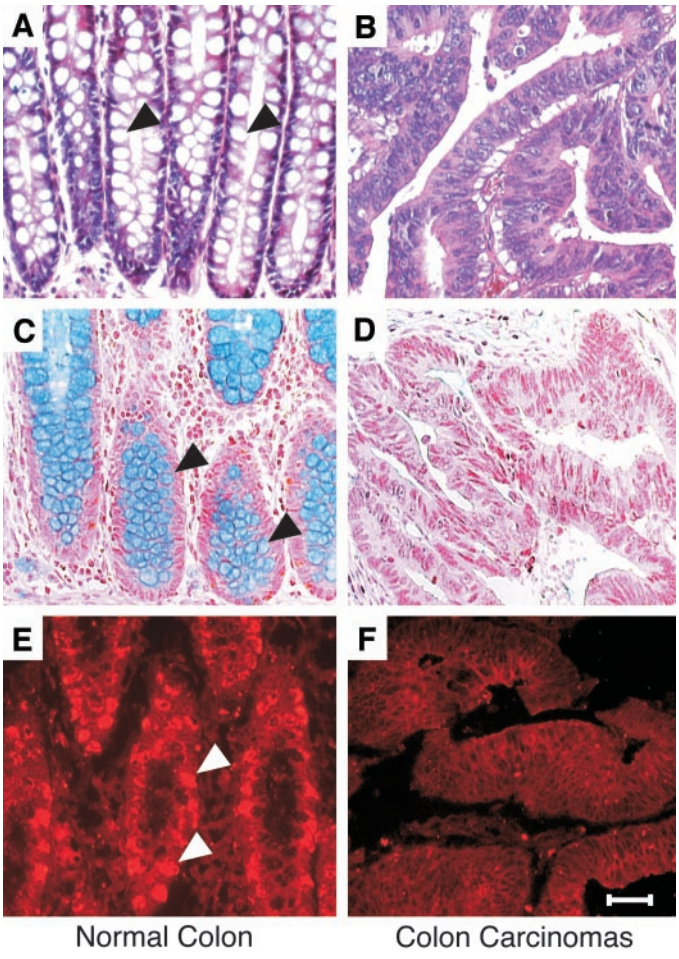

Fig. 1. Marked reduction of goblet cell populations in colon carcinomas. Sections of paraffin-embedded tissues from normal colon (*A*, *C*, and *E*) and colon adenocarcinomas (*B*, *D*, and *F*) are stained with H&E (*A* and *B*), Alcian blue (*C* and *D*), and MUC2 protein expression is detected by immunofluorescence (*E* and *F*). It is evident that the three methods of identifying goblet cells consistently reveal that although there is an abundance of goblet cells in the normal colon (*black* and *white arrowheads*), the number of goblet cells in colon adenocarcinomas is extremely low. Bar in *F* is 50 μm.

goblet cells, we performed anti-MUC2 immunofluorescent staining to compare goblet cells in normal colon *versus* colon adenocarcinoma (29). Results show that there were abundant goblet cells lining the normal colonic crypt (white arrowhead, Fig. 1*E*) but not in sections from colon adenocarcinoma (Fig. 1*F*). Examination of 18 samples by histochemical and immunohistochemical methods revealed reduced numbers of goblet cells in colon adenocarcinoma sections compared with their matched normal colon.

Hath1 Expression Is Repressed in Colorectal Tumor Tissue and Colorectal Cell Lines. To determine the role for Hath1 in colon cancer, we searched the Gene Logic database for altered expression of *Hath1* in various types of normal *versus* tumor tissue samples. This subscription-based Gene Logic database consists of expression data for normal (number of samples ranged from 22 to 914 depending on tissue type; see Supplemental Data) and tumor (number of tumor samples ranged from 6 to 290; see Supplemental Data) tissue determined by Affymetrix microarray analyses. The results revealed that *Hath1* expression in normal tissues was highest in colon (270 samples) and small intestine (177 samples) but relatively low in other tissues (Fig. 2). More importantly, *Hath1* expression was down-regulated in neoplastic tissues originating from colon (178 samples) and small intestine (15 samples). In contrast, tissues such as breast, liver, and prostate did not show differential *Hath1* expression, whereas *Hath1* expression appeared to be slightly elevated in endometrial and stomach cancers.

We next examined *Hath1* expression in clinical colon tumor samples and colorectal cancer cell lines using quantitative TaqMan real-time reverse transcription-PCR analysis. Total RNA of colorectal tumor and matched normal colon tissues were obtained from 12 different patients. The 12 colon tumor samples were classified as invasive colorectal adenocarcinoma except for sample 6, which was the only case classified as mucinous colon adenocarcinoma (a rare subtype of colorectal adenocarcinoma). Interestingly, *Hath1* expression was significantly (Student's *t* test, $P < 0.001$) down-regulated in all of the samples except for sample 6 (Fig. 3*A*). We then examined *Hath1* gene expression in total RNA obtained from various colon cancer cell lines. Compared with normal small intestine and colon, we detected only minimal *Hath1* expression in all of the colon cancer cell lines except for slightly elevated levels in the LS174T cell line (Fig. 3*B*).

Given that *Hath1* mRNA expression was significantly reduced in multiple colon adenocarcinomas, which contained few goblet cells, we wanted to examine the spatial expression pattern of Hath1 protein in the same set of colon adenocarcinoma tissue array by immunohistochemistry. Eighteen samples of colon adenocarcinoma and their corresponding matched normal colon sections in a tissue microarray were examined for Hath1 protein expression pattern. Here we observed specific localization of Hath1 protein expression in a considerable number of goblet cells in normal colon tissue sections (black arrow, Fig. 3*C1*). However, in adjacent tumor sections from matched patients, which were easily identifiable by the presence of highly elongated nucleus and disorganized and crowded cells, Hath1-positive staining was greatly reduced and in many cases completely absent (Fig. 3*C2*). Anti-Math1 antibody from two different sources and a second set of tissue arrays from NxGen Biosciences (San Diego, CA) produced reproducible Hath1 staining pattern (data not shown).

To examine Hath1 expression with respect to proliferating, Ki67-positive cells, we double-labeled the tissue arrays described previously with anti-Math1 and anti-Ki67. We detected a moderate number of Ki67-positive cells in normal colon sections (Fig. 3*C3*); however, the number of Ki67-positive cells was greatly enhanced in colon

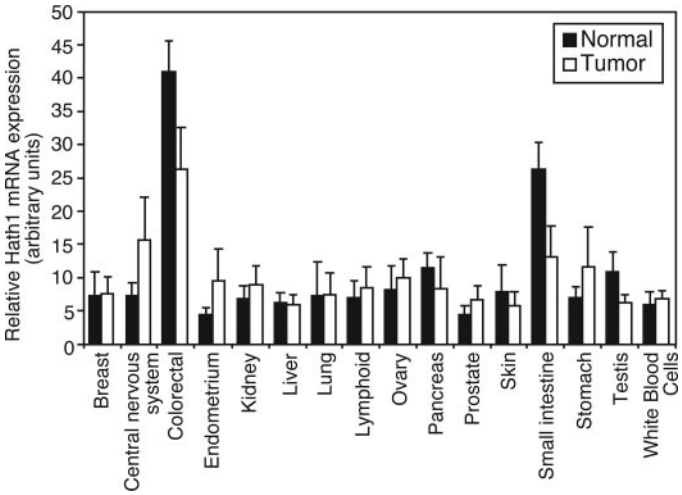

Fig. 2. Expression of Hath1 in various types of normal and tumor tissues. Expression of Hath1 in various tissue samples from the subscription-based Gene Logic database. Note that Hath1 expression is selectively high in normal colon and small intestine but reduced in colon and small intestinal tumors. In contrast, Hath1 expression is relatively low in other normal tissues with little or no differential expression of Hath1 between normal and tumor tissues in other organs such as breast, lung, and liver.

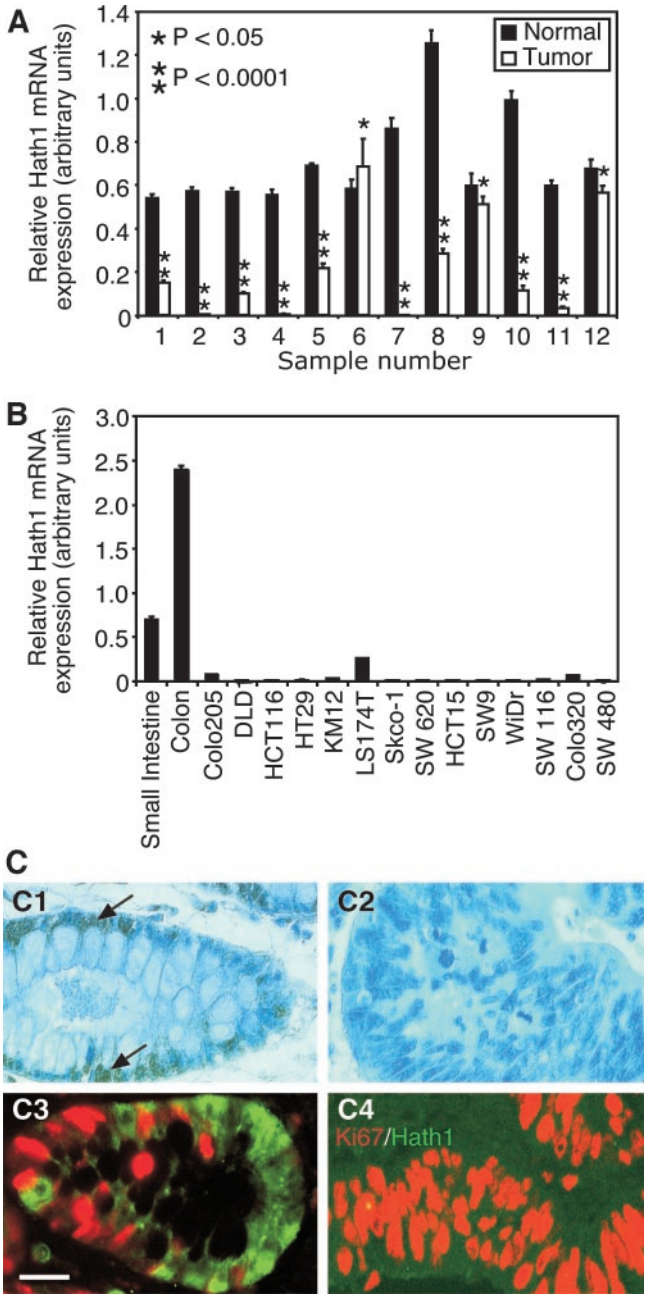

Fig. 3. Down-regulation of Hath1 in colon carcinomas. *A*, Hath1 mRNA expression in paired clinical normal human colon and colon tumor samples. Quantitative real-time (TaqMan) reverse transcription-PCR analysis of Hath1 mRNA expression was performed on paired normal *versus* colon tumor tissues. Data were plotted as relative Hath1 mRNA expression following normalization with RPL19, a housekeeping gene. *B*, Hath1 mRNA expression in tissues from normal intestinal tissue *versus* multiple colon cancer cell lines. Quantitative real-time (TaqMan) reverse transcription-PCR analysis of Hath1 expression was performed on total RNA isolated from tissues and colon cancer cell lines. Data are plotted as relative Hath1 mRNA expression following RPL19 normalization. *C*, immunohistochemical detection of Hath1 in normal human colon and colon adenocarcinoma. Immunohistochemistry of paraffin-embedded tissue sections was performed using anti-Math1 antibody, previously shown to recognize Hath1 protein (17). Shown are representative images obtained from a normal colon (*C1*) and a colon tumor (*C2*) samples from the tissue array. Note that Hath1 was expressed in a considerable number of goblet cells (*black arrow*) in normal colon, but few, if any, can be detected in colon adenocarcinomas. Hath1 expression (*green*) in normal colon did not coincide with proliferating, Ki67-expressing cells (*red*; *C3*). In tumors, there was an abundance of Ki67-positive cells (*red*), but no Hath1 expression was detected (*C4*); bar in *C3*, 100 μm.

adenocarcinoma (Fig. 3*C4*). A majority of Hath1-positive cells also were not Ki67 positive in 24 normal colons examined (Fig. 3*C3*). In colon adenocarcinoma, Hath1 expression was absent from multiple cases examined (Fig. 3*C4*).

Hath1 Inhibits Proliferation of Colorectal Cancer Cell Lines. To determine whether introduction of Hath1 would alter the proliferative ability of colon cancer cells, HT29 colon cancer cells were transfected with either pcDNA3.1 or pcDNA3.1 Hath1. Following G418 selection, two clones were randomly chosen from each transfection and subjected to quantitative real-time reverse transcription-PCR analysis to determine the level of Hath1 expression in these two clones. We found that the level of Hath1 expression in clone 4 was ~104-fold and clone 9 was ~22-fold above endogenous Hath1 expression in pcDNA3.1-transfected HT29 cells (data not shown). Because the two randomly selected clones showed levels of Hath1 above endogenous level, we continued with characterization of these two clones. First, tritiated-thymidine ([^{3}H]thymidine) incorporation assay was performed on these stable HT29 cell lines to determine their proliferative ability. HT29 clones stably overexpressing Hath1 incorporated less [^{3}H]thymidine compared with clones transfected with pcDNA3.1 ($P < 0.001$; see also Colony Formation Assay below; Fig. 4*A*). Supplementary to the [^{3}H]thymidine-incorporation assay, we used a second method to evaluate DNA synthesis (*i.e.*, immunofluorescent staining on cells that had incorporated the thymidine analog BrdUrd. Cell counts of BrdUrd-positive cells *versus* total number of cells, assessed through DAPI nuclear staining, revealed significantly ($P < 0.0001$) fewer BrdUrd-positive cell in HT29 cells stably expressing Hath1 than the clones transfected with pcDNA3.1 (Fig. 4*B* and *C*). Considering that the high level of Hath1 expression was different from Hath1 expression in colon tumor *versus* normal colon (Fig. 3*A*), it was possible that the decreased proliferation seen in Hath1-expressing clones (Fig. 4*A–C*) was caused by the toxic effect of Hath1 overexpression. To address this issue, we performed caspase-3 staining and found that there was no increased cell death in the Hath1-expressing clones compared with clones transfected with pcDNA3.1 (data not shown). Furthermore, the DAPI-stained nuclei did not display apoptotic characteristics (Fig. 4*B*).

Hath1 Can Suppress Anchorage-Independent Growth of HT29 Colon Cancer Cells in Soft Agar and Xenografts in Athymic Nude Mice. In our efforts to determine the effect of Hath1 expression on anchorage-independent growth of HT29 colon cancer cells, we performed colony formation assay in soft agar. After 10 days in culture, we found that HT29 cell lines stably expressing pcDNA3.1 Hath1 (clone 4 and clone 9) formed colonies that were minute compared with HT29 pcDNA3.1 cell lines (clone 2 and clone 3; Fig. 5*A*). More importantly, counting of all of the visible colonies revealed that there was an approximately 10-fold reduction in the number of colonies formed ($n = 3$; $P < 0.001$) from HT29 cells stably expressing pcDNA3.1 Hath1 (Fig. 5*B*).

We extended our study by assessing the growth of these HT29 stable clones in a xenograft experiment. HT29 stably transfected cells were injected s.c. into athymic nude mice and monitored for tumor growth. Twenty days after xenograft, tumor formation of HT29 cells expressing Hath1 (clones 4 and 9) were significantly inhibited ($P < 0.01$; Fig. 5*C*). It also is important to emphasize here that two mice injected with HT29 cells expressing pcDNA3.1 Hath1 (clone 4) displayed no tumor growth 20 days after xenograft. This was true even after extending the study for another 12 days. By this later time point, untransfected and pcDNA3.1-transfected (clone 3) HT29 cells continued to grow robustly compared with Hath1-expressing clones (clone 4, $P < 0.01$; clone 9, $P < 0.05$; Fig. 5*C*).

Hath1 Induces Expression of MUC2, a Marker for Goblet Cell Differentiation, in HT29 Colorectal Cancer Cell Line. Because Math1 has been implicated in inducing differentiation of intestinal epithelial cells (13), we questioned whether inhibition of proliferation (Fig. 4) could be attributable to Hath1 driving progenitor cells into terminal differentiation in colon cancer cells. Hence, we examined the

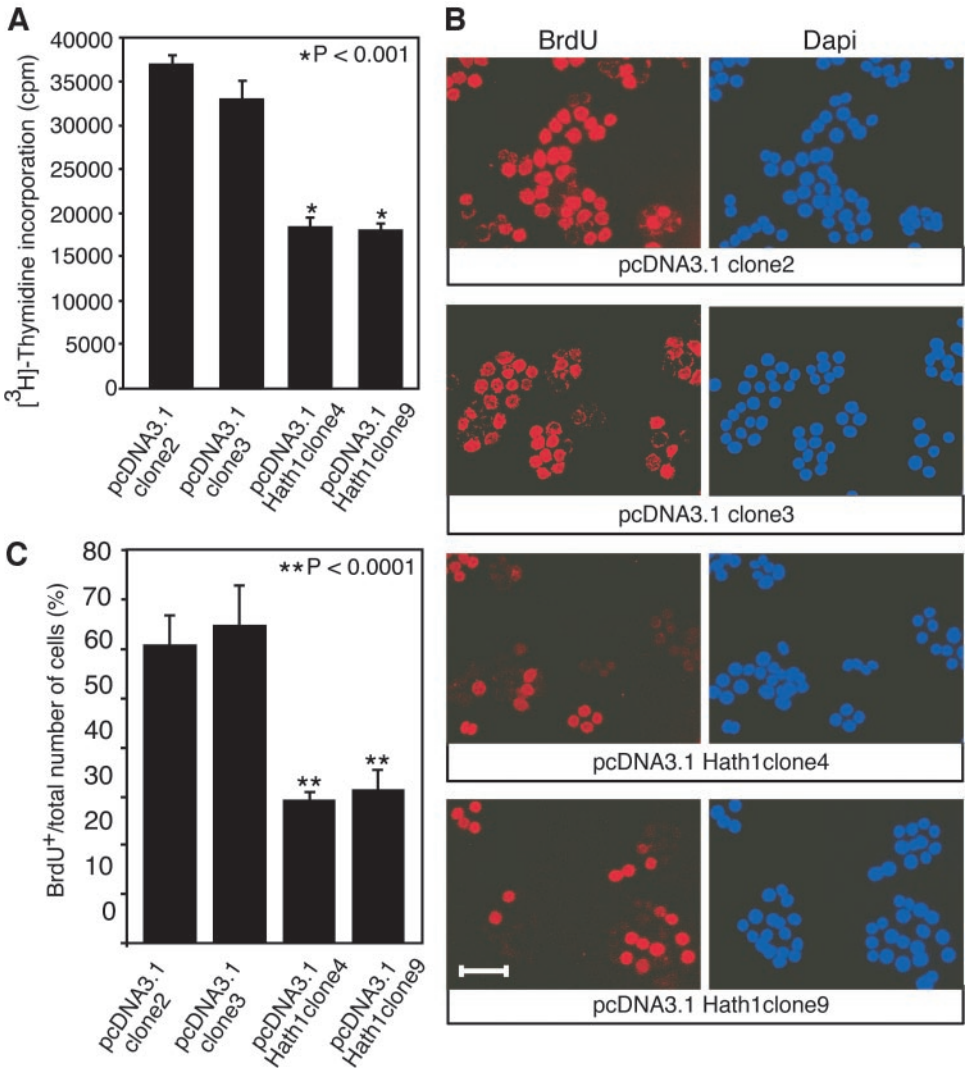

Fig. 4. Overexpression of Hath1 inhibits proliferation of colon cancer cells. *A*, analysis of Hath1 overexpression effect on DNA synthesis of colon cancer cells. [^{3}H]thymidine incorporation assay was used to determine the effect of Hath1 on cell proliferation. Twenty-four hours after splitting HT29 colon cancer cells stably expressing either pcDNA3.1 or pcDNA3.1 Hath1, [^{3}H]thymidine was added for 16 hours. Data were collected from 24 culture wells from each of the experimental groups and were expressed as mean ± SD. *B*, immunofluorescent staining of HT29-transfected cells for BrdUrd. Analysis of HT29 colon cancer cells were stably transfected with either pcDNA3.1 (clone 2 and clone 3) or pcDNA3.1 Hath1 (clone 4 or clone 9). Cells then were labeled using mouse anti-BrdUrd and immunofluorescently detected using antimouse rhodamine-conjugate. Cells also were DAPI-stained to identify total number of cells; bar in *B* is 60 μm. *C*, quantitation of BrdUrd-positive cells. Results of cell count are presented as a percentage of BrdUrd-positive cells *versus* total number of DAPI-positive cells. Fifteen different fields were randomly selected for analysis from triplicates of HT29 stable clones with either pcDNA3.1 or pcDNA3.1 Hath1. Data were plotted as mean ± SD, and two-way, unpaired Student's *t* test was used for statistical analysis.

expression of MUC2, a marker of goblet cell differentiation, by Western blot analysis following forced expression of Hath1 in HT29. As shown in Fig. 6*A*, MUC2 protein expression was significantly up-regulated in HT29 cells transfected with pcDNA3.1 Hath1 (clone 4 and clone 9).

Active Wnt Signaling Represses Hath1 in Colorectal Cell Lines. Given that Hath1 could induce MUC2 expression and MUC2 was a target gene of Wnt regulation (30), we examined whether Hath1 also was under Wnt regulation during colon tumorigenesis in HT29 colon cancer cells. Because HT29 colorectal cells are known to possess APC mutation (31), we inhibited Wnt signaling through transient expression of wild-type APC (pcDNA3 APC2) and dominant negative lymphocyte enhancer factor (pcDNA3 Lef1^{DN}; refs. 30, 32, 33). Using Topflash luciferase assay (Upstate Biotechnology, Lake Placid, NY) 48 hours after transfection, we observed that transient expression of pcDNA3 APC2 and pcDNA3 Lef1^{DN} could inhibit Wnt signaling in HT29 cells (Fig. 6*B*). We found that such inhibition of Wnt signaling in HT29 cells was capable of MUC2 induction (Fig. 6*C*). Taqman reverse transcription-PCR analysis also revealed that *Hath1* expression increased significantly in HT29 cells ($P < 0.01$) once Wnt signaling was inhibited with either wild-type APC or dominant negative Lef1 (Fig. 6*D*).

Overexpression of Hath1 Leads to Down-Regulation of Cyclin D1 and Up-Regulation of p27. To investigate whether the ability of Hath1 to induce differentiation was mediated by one or more cell cycle checkpoint regulators, we decided to examine the expression of cyclin D1, which is a key cell cycle regulator and also a direct target of Wnt signaling (34–36). Western blot analysis of cyclin D1 revealed that expression of cyclin D1 was down-regulated in HT29 cells stably expressing Hath1 compared with HT29 cells transfected with pcDNA3.1 (Fig. 7*A*). We then decided to examine the expression of p27 because it has been associated with intestinal adenomas and known to influence goblet cell differentiation (24, 37–39). By Western blot analysis, expression of p27 was elevated as a result of Hath1 overexpression (Fig. 7*B*).

DISCUSSION

The data presented in this study show that Hath1 can inhibit cell proliferation, induce a goblet cell differentiation marker, MUC2, in colon cancer cell line, suppress anchorage-independent growth of colon cancer cells in a soft agar colony formation assay, and, more significantly, inhibit growth of HT29 colon cancer cells in xenograft experiments. Yang *et al.* (13) previously showed that *Math1* was essential for differentiation of various secretory epithelial cells in the intestine, one of which are goblet cells. Goblet cells are the same cells that we and others find either reduced or absent in clinical samples of colon adenocarcinoma (4, 5). Because *Math1* null mice die shortly after birth, this precludes the study of *Math1* in colon tumorigenesis in these mice. Hence, our study bridges the role of Hath1 in goblet cell differentiation and the frequently observed

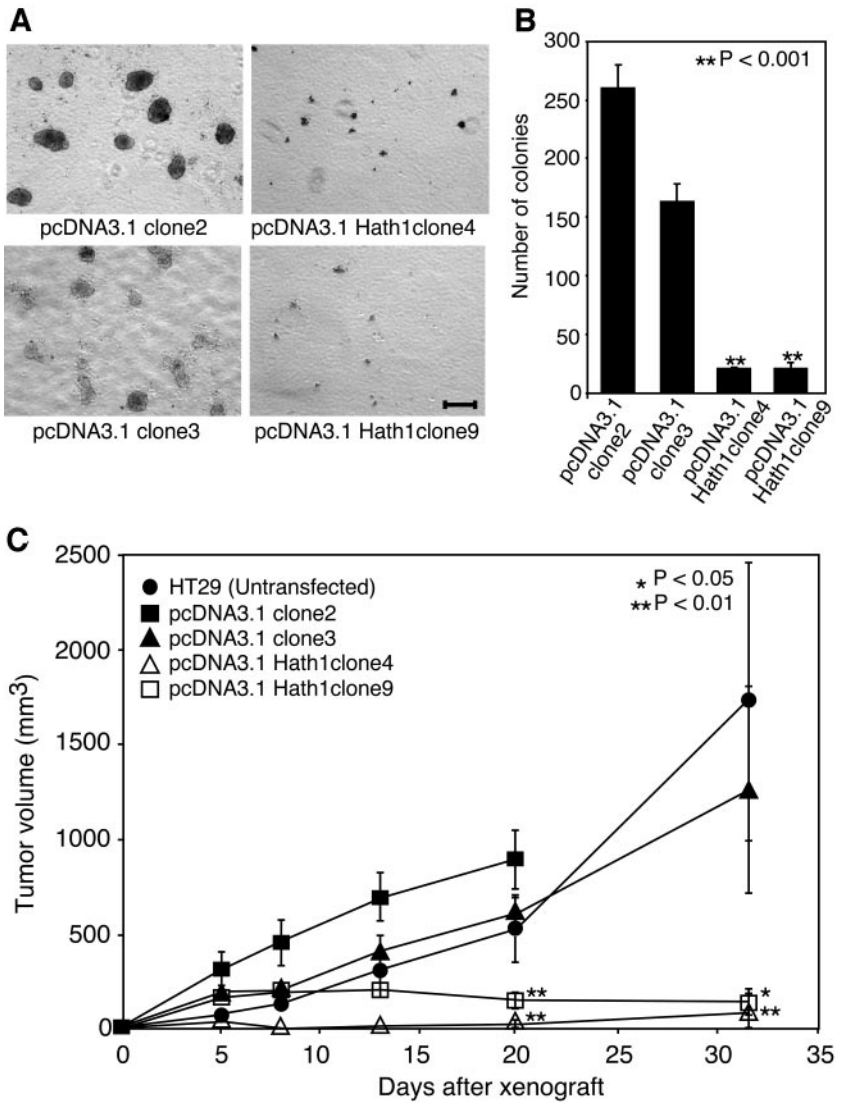

Fig. 5. Hath1 suppresses anchorage-independent growth and xenograft of HT29 colon cancer cells. *A*, micrographs of HT29 colon cancer cells stably expressing control vector pcDNA3.1 or pcDNA3.1Hath1. Note that the size of colonies originating from control vector HT29 clones are markedly bigger compared with stable clones overexpressing Hath1; *bar*, 400 μm. *B*, colony formation assay on HT29 stably expressing pcDNA3.1 (clone 2 and clone 3) and pcDNA3.1 Hath1 (clone 4 and clone 9). The assay was performed in triplicate, and colonies were counted from multiple, randomly selected fields. Note that the number of colonies in the Hath1-expressing cells is significantly lower than HT29 transfected with pcDNA3.1. *C*, Xenograft of HT29 stably expressing pcDNA3.1 (clone 2 and clone 3) and pcDNA3.1 Hath1 (clone 4 and clone 9) measured during a 32-day period. Mice injected with pcDNA3.1 (clone 2) were sacrificed before 32 days because of large tumor burden or signs of impending tumor ulceration. Tumor growth in untransfected and pcDNA3.1-expressing HT29 cells were robust compared with those expressing pcDNA3.1 Hath1. Data were plotted as mean ± SEM, and ANOVA was used for statistical analysis.

reduction of goblet cells in colon adenocarcinomas to present a clear involvement of Hath1 in colon cancer.

In addition to Math1, other neurogenic bHLH transcription factors downstream of the Notch signaling pathway, including Hes1, NeuroD, and Neurogenin3, have been reported to play a role in cell fate determination of the intestine. For example, NeuroD and Neurogenin3 were reported to regulate cell fate specification of the intestinal endocrine cells (40, 41). Null mutant mice of Hes1, which is a bHLH transcriptional repressor rather than a bHLH transcriptional activator (Math1), produced excessive goblet cells in the intestine (42). Jensen *et al.* (42) also showed that removal of Hes1 activity resulted in elevated expression of Math1. Co-electroporation of Hes1 and Math1 into the inner ear tissue also can block hair cell differentiation induced by Math1 (16). These studies suggest that Hes1 also may potentially antagonize Hath1 activity during colon epithelial development, but the significance of such an antagonistic relationship remains to be determined.

One notable finding in our study is the role of Hath1 in colon tumorigenesis. This is supported, in part, by our examination of Hath1 expression in colon tumor samples. Initial analysis of data retrieved from the Gene Logic database revealed that Hath1 expression was down-regulated in colon tumor but not in other tissue types (Fig. 2). However, Hath1 expression is moderately elevated in endometrial and stomach tumors. Coincidentally, the former is known to be mucinous, and the latter often contains goblet cells and gland structure (43–45). Further studies would be necessary to investigate whether Hath1 too plays a role in the progression of endometrial and stomach tumors. It is interesting to note that in Fig. 3*B*, Hath1 expression appeared to be moderately expressed in LS174T colon cancer cell line, which has been shown by others to express MUC2 (46). Consistent with this observation, we detected Hath1 expression in a considerable number of goblet cells, and most Hath1-positive cell population did not colocalize with Ki67-expressing cells in normal human colonic epithelium (Fig. 3*C3*). In contrast, we detected few, if any, Hath1-positive cells in colon adenocarcinoma tissues, which suggests a potential role for loss of Hath1 in colon tumorigenesis (Fig. 3*C4*). Yang *et al.* (13) reported Math1 expression in goblet cells, enteroendocrine cells, and Paneth cells in mouse intestine and colon, with Ki67/Math1 colocalization in some but not all progenitor cells. However, our analyses of 24 normal human colon tissues revealed that a majority of Hath1-positive cells did not colocalize with Ki67-positive cells even though they appeared in the vicinity of Ki67-positive cells. It is possible that in normal human colon, Hath1 is expressed in cells that have just completed terminal mitosis and, thus, does not colocalize with actively proliferating cells. Such a requirement for Hath1 immediately after cells have exited the cell cycle also has been shown previously in the inner ear, where Math1 expression is essential only for cells that have just exited the

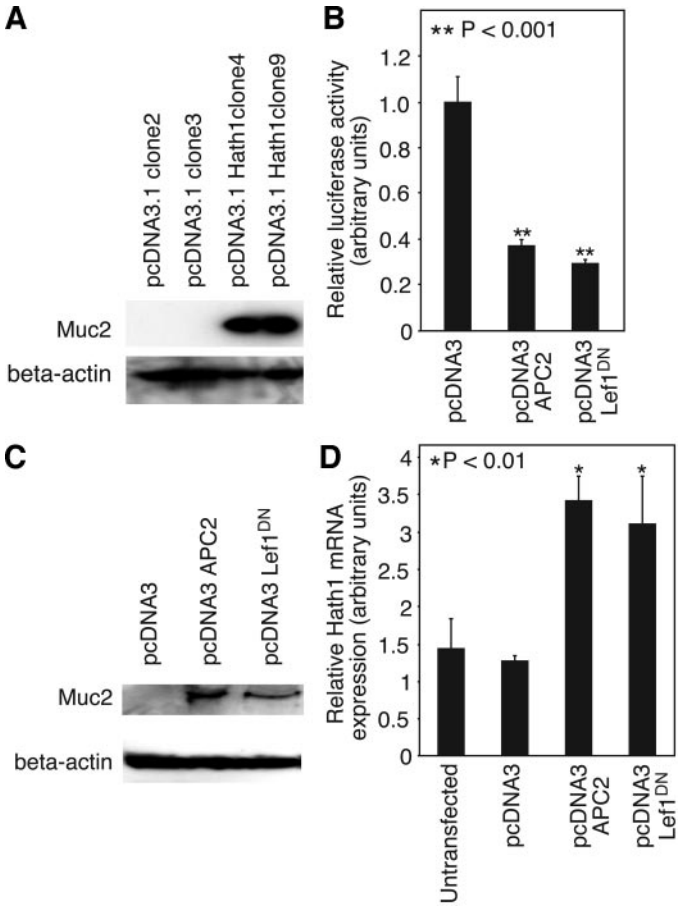

Fig. 6. Expression of Hath1 up-regulates MUC2 protein, and inhibition of Wnt elevates expression of *Hath1* and MUC2. *A*, MUC2 protein expression by Western blot analysis. HT29 stably expressing pcDNA3.1 Hath1 (clone 4 and clone 9) can induce MUC2 expression, whereas HT29 cells stably expressing pcDNA3.1 (clone 2 and clone 3) do not induce MUC2 expression. *B*, Topflash luciferase assay of pcDNA3, pcDNA APC2, and pcDNA Lef1^{DN}. Wnt signaling is inhibited on expression of APC2 and Lef1^{DN}. *C*, MUC2 protein expression by Western blot analysis as a result of Wnt inhibition. Protein lysates from HT29 transfected with pcDNA APC2 or pcDNA Lef1^{DN} were transferred onto polyvinylidene difluoride membrane and incubated with anti-MUC2 monoclonal antibody. MUC2 expression was increased on inhibition of Wnt signaling. *D*, Inactivation of Wnt leads to up-regulation of *Hath1*. Quantitative TaqMan reverse transcription-PCR analysis of Hath1 expression in HT29 colon cancer cells transfected with pcDNA APC2 or pcDNA Lef1^{DN}. Expression of Hath1 was noticeably enhanced in cells in which Wnt signaling had been inhibited.

cell cycle to form a zone of nonproliferating cells during normal development (47).

Our data showing Hath1 inhibition of cell proliferation and induction MUC2 is in agreement with previous work on Hath1 in the brain and inner ear (Fig. 4 and Fig. 6*A*). For example, misexpression of Math1 leads to production of supernumerary, terminally differentiated hair cells in the inner ear (16–18). Similarly, Math1 expression also defines differentiation of brain neurons and spinal cord commissural interneurons in the developing nervous system (10, 48). Furthermore, targeted deletion of Math1 results in a failure for cerebellar granule neurons and inner ear hair cells to differentiate (14, 15). The Hath1 suppressive effect on proliferation of colon cancer cells is not only limited to *in vitro* soft agar colony formation assay but also *in vivo* xenograft experiments (Fig. 5).

Our results show that Hath1 may be negatively regulated by Wnt signaling, a pathway critical in colon tumor progression (Fig. 6*D*). We generally found Hath1 expression to be extremely low in all of the colon cancer cell lines, which coincidentally have constitutively active Wnt signaling. Although direct interaction between TCF/Lef transcription factors and Hath1 promoter has not been reported, we did find core TCF/Lef-binding site (5′-A/T A/T CAAAG-3′) in the Hath1 promoter located 2904 bp upstream of the translation initiation site (data not shown). Consistent with our findings, a recent microarray study examining the gene expression profile of inhibition of Wnt signaling in LS174T colon cancer cells revealed that expression of MUC2 was elevated when Wnt signaling was inhibited (30). A study by Pretlow *et al.* (49) showed that APC mutations are involved in the initiation of aberrant crypt foci, which are precursors to adenoma and colon adenocarcinoma. Goblet cells were already absent from aberrant crypt foci (50). Together, it is possible that the loss of Hath1 expression in aberrant crypt foci may represent an early event in tumorigenesis.

Although we find that Hath1 is negatively regulated by Wnt, Pinto *et al.* (51) reported that intestines of transgenic mice ectopically expressing Dickkopf1 (Dkk1) lacked goblet cells and Math1 expression. This inconsistency with our findings could be a result of broader Wnt inhibition by Dkk1, which encompasses canonical and noncanonical Wnt signaling pathways such as Wnt/Ca^{+} pathway and planar polarity/c-Jun NH_2-terminal kinase pathway (reviewed in refs. 52–54). Conversely, van de Wetering *et al.* (30) showed that inhibition of Wnt signaling by dominant negative Tcf4 in LS174T colon cancer cells resulted in elevated MUC2 expression, which is consistent with our observation of enhanced MUC2 expression on inhibition of Wnt signaling. Pinto *et al.* (51) reported that Math1 expression and goblet cells were maintained in Tcf4-deficient mice. Hence, it would be interesting to determine in future studies whether Hath1 expression also could be enhanced in LS174T cells expressing dominant negative Tcf4. It is possible that Wnt regulation of MUC2 and Hath1 may be different in normal colon as compared with colon adenocarcinoma environment. Recently, Ireland *et al*. demonstrated that inhibition of β-catenin resulted in goblet cell depletion, which supports our findings (55).

Given the involvement of cycle checkpoint regulators during cancer progression, our results also show that Hath1 positively regulates p27 but negatively regulates cyclin D1 (Fig. 7; refs. 34, 56, 57). Hence, decrease in cell proliferation as a result of Hath1 overexpression in our studies could be attributed to a reduction in cyclin D1. Conversely, overexpression of p27 as a result of Hath1 overexpression could potentially facilitate cell cycle exit, consequently allowing Hath1 to induce differentiation of colon cancer cells. Although Tetsu and McCormick (58) reported that overexpression of p27 and the eventual repression of cdk2 was not sufficient to cause growth arrest in several colorectal cancer cell lines, reduction of p27 in tumors often correlates with tumor aggressiveness and eventually results in poor patient prognosis and a poor state of differentiation (59). Yang *et al.*

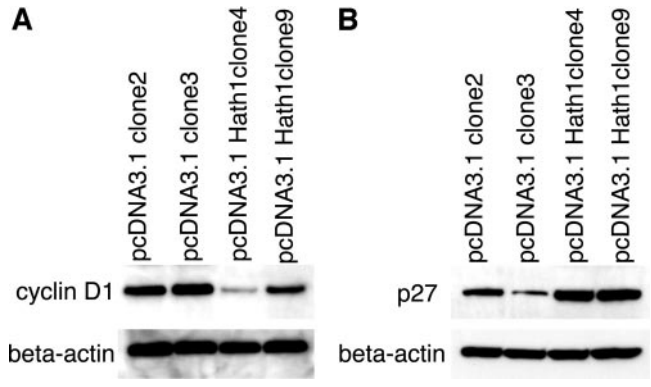

Fig. 7. Hath1 suppresses expression of cyclin D1 but up-regulates p27 expression. *A*, Western blot analysis of cyclin D1 in stable HT29 colon cancer cell lines expressing Hath1 or control vector. Two clones were analyzed from each category for cyclin D1 expression, and β-actin was used as internal loading control. Note that cyclin D1 expression was reduced in HT29 clones stably expressing Hath1. *B*, expression of p27 protein by Western blot analysis HT29 colon cancer cells. Level of p27 expression was up-regulated in HT29 cells Hath1 but markedly reduced in HT29 cells expressing pcDNA3.1.

(24) showed that inactivation of p27 alone was sufficient to induce the formation of small and large intestinal adenomas. Interestingly, these adenomas also displayed reduced goblet cell differentiation, revealed by Alcian blue staining and MUC2 expression, thereby suggesting that p27 was important for maintenance of intestinal homeostasis (59). However, the mechanistic role of p27 in colon cancer is unclear and requires more study.

In conclusion, this is the first study to show the role of Hath1 in colon tumorigenesis. We show that down-regulation of Hathl can result in reduced expression of goblet cell differentiation marker, MUC2, which contributes toward the progression of neoplastic growth. This study also identifies *Hath1* as a novel gene that may be downstream of Wnt regulation, which is well documented in colon cancer.

ACKNOWLEDGMENTS

We thank Hartmut Koeppen for his instrumental input and helpful discussions for colon cancer pathology, and Zemin Zhang for his tremendous help in the area of bioinformatics. We also thank Ralph Schwall, Ayly Ling Tucker, Bonnee Rubinfeld, Gail Lewis Phillip, Dineli Wickramasinghe, and Alex Abbas for discussions, and Allison Bruce for assistance with preparation of the figures.

REFERENCES

1. Jemal A, Murray T, Samuels A, Ghafoor A, Ward E, Thun MJ. Cancer statistics, 2003. CA Cancer J Clin 2003;53:5–26.
2. Jemal A, Thomas A, Murray T, Thun M. Cancer statistics, 2002. CA Cancer J Clin 2002;52:23–47.
3. Augenlicht L, Velcich A, Mariadason J, Bordonaro M, Heerdt B. Colonic cell proliferation, differentiation, and apoptosis. Adv Exp Med Biol 1999;470:15–22.
4. Hanski C, Riede E, Gratchev A, et al. MUC2 gene suppression in human colorectal carcinomas and their metastases: in vitro evidence of the modulatory role of DNA methylation. Lab Invest 1997;77:685–95.
5. Ho SB, Niehans GA, Lyftogt C, et al. Heterogeneity of mucin gene expression in normal and neoplastic tissues. Cancer Res 1993;53:641–51.
6. Audie JP, Janin A, Porchet N, Copin MC, Gosselin B, Aubert JP. Expression of human mucin genes in respiratory, digestive, and reproductive tracts ascertained by in situ hybridization. J Histochem Cytochem 1993;41:1479–85.
7. Sylvester PA, Myerscough N, Warren BF, et al. Differential expression of the chromosome 11 mucin genes in colorectal cancer. J Pathol 2001;195:327–35.
8. Velcich A, Yang W, Heyer J, et al. Colorectal cancer in mice genetically deficient in the mucin Muc2. Science 2002;295:1726–9.
9. Akazawa C, Ishibashi M, Shimizu C, Nakanishi S, Kageyama R. A mammalian helix-loop-helix factor structurally related to the product of Drosophila proneural gene atonal is a positive transcriptional regulator expressed in the developing nervous system. J Biol Chem 1995;270:8730–8.
10. Helms AW, Johnson JE. Progenitors of dorsal commissural interneurons are defined by MATH1 expression. Development 1998;125:919–28.
11. Isaka F, Ishibashi M, Taki W, Hashimoto N, Nakanishi S, Kageyama R. Ectopic expression of the bHLH gene Math1 disturbs neural development. Eur J Neurosci 1999;11:2582–8.
12. Ben-Arie N, Hassan BA, Bermingham NA, et al. Functional conservation of atonal and Math1 in the CNS and PNS. Development 2000;127:1039–48.
13. Yang Q, Bermingham NA, Finegold MJ, Zoghbi HY. Requirement of Math1 for secretory cell lineage commitment in the mouse intestine. Science 2001;294:2155–8.
14. Ben-Arie N, Bellen HJ, Armstrong DL, et al. Math1 is essential for genesis of cerebellar granule neurons. Nature 1997;390:169–72.
15. Bermingham NA, Hassan BA, Price SD, et al. Math1: an essential gene for the generation of inner ear hair cells. Science 1999;284:1837–41.
16. Zheng JL, Gao WQ. Overexpression of Math1 induces robust production of extra hair cells in postnatal rat inner ears. Nat Neurosci 2000;3:580–6.
17. Shou J, Zheng JL, Gao WQ. Robust generation of new hair cells in the mature mammalian inner ear by adenoviral expression of Hath1. Mol Cell Neurosci 2003; 23:169–79.
18. Kawamoto K, Ishimoto S, Minoda R, Brough DE, Raphael Y. Math1 gene transfer generates new cochlear hair cells in mature guinea pigs in vivo. J Neurosci 2003;23: 4395–400.
19. Bienz M, Clevers H. Linking colorectal cancer to Wnt signaling. Cell 2000;103:311–20.
20. Oving IM, Clevers HC. Molecular causes of colon cancer. Eur J Clin Invest 2002; 32:448–57.
21. Polakis P. Wnt signaling and cancer. Genes Dev 2000;14:1837–51.
22. Markowitz SD, Dawson DM, Willis J, Willson JK. Focus on colon cancer. Cancer Cell 2002;1:233–6.
23. McKay JA, Douglas JJ, Ross VG, et al. Analysis of key cell-cycle checkpoint proteins in colorectal tumours. J Pathol 2002;196:386–93.
24. Yang W, Bancroft L, Nicholas C, Lozonschi I, Augenlicht LH. Targeted inactivation of p27kip1 is sufficient for large and small intestinal tumorigenesis in the mouse, which can be augmented by a Western-style high-risk diet. Cancer Res 2003;63: 4990–6.
25. Yang W, Velcich A, Mariadason J, et al. p21(WAF1/cip1) is an important determinant of intestinal cell response to sulindac in vitro and in vivo. Cancer Res 2001;61: 6297–302.
26. Sutter T, Doi S, Carnevale KA, Arber N, Weinstein IB. Expression of cyclins D1 and E in human colon adenocarcinomas. J Med 1997;28:285–309.
27. Gibson UE, Heid CA, Williams PM. A novel method for real time quantitative RT-PCR. Genome Res 1996;6:995–1001.
28. Gaffney E. Laboratory Methods in Histotechnology. Washington DC: American Registry of Pathology; 1994.
29. Lee HW, Ahn DH, Crawley SC, et al. Phorbol 12-myristate 13-acetate up-regulates the transcription of MUC2 intestinal mucin via Ras, ERK, and NF-κ B. J Biol Chem 2002;277:32624–31.
30. van de Wetering M, Sancho E, Verweij C, et al. The β-catenin/TCF-4 complex imposes a crypt progenitor phenotype on colorectal cancer cells. Cell 2002;111:241–50.
31. Ilyas M, Tomlinson IP, Rowan A, Pignatelli M, Bodmer WF. β-catenin mutations in cell lines established from human colorectal cancers. Proc Natl Acad Sci USA 1997;94:10330–4.
32. Rubinfeld B, Souza B, Albert I, Munemitsu S, Polakis P. The APC protein and E-cadherin form similar but independent complexes with α-catenin, β-catenin, and plakoglobin. J Biol Chem 1995;270:5549–55.
33. Munemitsu S, Albert I, Souza B, Rubinfeld B, Polakis P. Regulation of intracellular β-catenin levels by the adenomatous polyposis coli (APC) tumor-suppressor protein. Proc Natl Acad Sci USA 1995;92:3046–50.
34. Sherr CJ. Cancer cell cycles. Science 1996;274:1672–7.
35. Shtutman M, Zhurinsky J, Simcha I, et al. The cyclin D1 gene is a target of the β-catenin/LEF-1 pathway. Proc Natl Acad Sci USA 1999;96:5522–7.
36. Tetsu O, McCormick F. β-catenin regulates expression of cyclin D1 in colon carcinoma cells. Nature 1999;398:422–6.
37. LaMont JT, O'Gorman TA. Experimental colon cancer. Gastroenterology 1978;75: 1157–69.
38. Philipp-Staheli J, Kim KH, Payne SR, et al. Pathway-specific tumor suppression. Reduction of p27 accelerates gastrointestinal tumorigenesis in Apc mutant mice, but not in Smad3 mutant mice. Cancer Cell 2002;1:355–68.
39. Ahnen DJ. Are animal models of colon cancer relevant to human disease. Dig Dis Sci 1985;30:103S–6S.
40. Apelqvist A, Li H, Sommer L, et al. Notch signalling controls pancreatic cell differentiation. Nature 1999;400:877–81.
41. Rindi G, Candusso ME, Solcia E. Molecular aspects of the endocrine tumours of the pancreas and the gastrointestinal tract. Ital J Gastroenterol Hepatol 1999;31(Suppl 2):S135–8.
42. Jensen J, Pedersen EE, Galante P, et al. Control of endodermal endocrine development by Hes-1. Nat Genet 2000;24:36–44.
43. Sivridis E, Giatromanolaki A, Koukourakis MI, Georgiou L, Anastasiadis P. Patterns of episialin/MUC1 expression in endometrial carcinomas and prognostic relevance. Histopathology 2002;40:92–100.
44. Zhao S, Hayasaka T, Osakabe M, et al. Mucin expression in nonneoplastic and neoplastic glandular epithelia of the uterine cervix. Int J Gynecol Pathol 2003;22: 393–7.
45. Fenoglio-Preiser CM, Noffsinger AE, Lantz PE, Stemmerman GN, Rilke FO. Gastrointestinal Pathology: An Atlas and Text. Philadelphia: Lippincott-Raven Publishers; 1999.
46. Matsuoka Y, Pascall JC, Brown KD. Quantitative analysis reveals differential expression of mucin (MUC2) and intestinal trefoil factor mRNAs along the longitudinal axis of rat intestine. Biochim Biophys Acta 1999;1489:336–44.
47. Chen P, Johnson JE, Zoghbi HY, Segil N. The role of Math1 in inner ear development: uncoupling the establishment of the sensory primordium from hair cell fate determination. Development 2002;129:2495–505.
48. Helms AW, Gowan K, Abney A, Savage T, Johnson JE. Overexpression of MATH1 disrupts the coordination of neural differentiation in cerebellum development. Mol Cell Neurosci 2001;17:671–82.
49. Pretlow TP, Edelmann W, Kucherlapati R, Pretlow TG, Augenlicht LH. Spontaneous aberrant crypt foci in Apc1638N mice with a mutant Apc allele. Am J Pathol 2003;163:1757–63.
50. Pretlow TP, Pretlow TG. Putative preneoplastic changes identified by enzyme histochemical and immunohistochemical techniques. J Histochem Cytochem 1998;46: 577–83.
51. Pinto D, Gregorieff A, Begthel H, Clevers H. Canonical Wnt signals are essential for homeostasis of the intestinal epithelium. Genes Dev 2003;17:1709–13.
52. van Es JH, Barker N, Clevers H. You Wnt some, you lose some: oncogenes in the Wnt signaling pathway. Curr Opin Genet Dev 2003;13:28–33.
53. Peifer M, Polakis P. Wnt signaling in oncogenesis and embryogenesis—a look outside the nucleus. Science 2000;287:1606–9.
54. Zorn AM. Wnt signalling: antagonistic Dickkopfs. Curr Biol 2001;11:R592–5.
55. Ireland H, Kemp R, Houghton C, et al. Inducible Cre-mediated control of gene expression in murine gastrointestinal tract: effect of loss of β-catenin. Gastroenterology 2004;126:1236–46
56. Hanahan D, Weinberg RA. The hallmarks of cancer. Cell 2000;100:57–70.
57. Sherr CJ. The Pezcoller lecture: cancer cell cycles revisited. Cancer Res 2000;60: 3689–95.
58. Tetsu O, McCormick F. Proliferation of cancer cells despite CDK2 inhibition. Cancer Cell 2003;3:233–45.
59. Blain SW, Scher HI, Cordon-Cardo C, Koff A. p27 as a target for cancer therapeutics. Cancer Cell 2003;3:111–5.